

Chaos and a quantitative modeling of the kinetics of phase transitions on the final measure areas

Ivan G. Grabar¹, Olga I. Grabar², Yuri O. Kubrak³, Mykola M. Marchuk⁴

¹ Zhytomyr National Agroecological University
Staryi Blvd 7, Zhytomyr, 10008 Ukraine
(E-mail: ivan-grabar@rambler.ru)

² Zhytomyr State Technological University
Cherniachovskiy 103, Zhytomyr, 10005 Ukraine
(E-mail: grabar-olga@rambler.ru)

³ Zhytomyr State Technological University
Cherniachovskiy 103, Zhytomyr, 10005 Ukraine
(E-mail: kubrak79@ukr.net)

⁴ National University of Water and Environment Management,
Soborna street 11, Rivne, 33028 Ukraine
(E-mail: m.m.marchuk@nuwm.edu.ua)

Abstract. The analysis of chaos role in the modeling the phase transition kinetics (percolation model, Ising's model, a model of melting nanoparticles) was shown.

It was discovered and quantitatively described the role of scale in these phase transitions (PT). On an example of the stochastic simulation algorithm of percolation it was shown that the final measure models is a number of features that define the region's large-scale constant L. Thus, with decreasing L:

- percolation threshold P^* increases;
- region scattering (band phase transition) increases;
- fractal dimension of nano-object is reduced.

The quantitative relationships of these parameters on a large-scale field constant L were established. It is shown that the probability of connecting cluster well described by Fermi-Dirac-Grabar distribution:

$$W(L) = 1 / (1 + \exp((P^* - P) / L)).$$

A functional dependence of threshold a percolation P^* from the fractal dimension of the space D (Cartesian approach prof. Grabar) was realised:

$$P^* = 1 - \ln((D + 1) / 2)$$

Keywords: Chaos, Phase transitions, Percolation, Percolation threshold, Fractal dimension, The clipping cluster.



1. Introduction

Simulation of percolation is used for quantitative studies of phase transitions and the study of nano-objects properties. Usually, phase transition means the instant change of system state with little change in the control parameters (Fig.1). Indeed, in percolation problems with the size of the area $L \rightarrow \infty$ holds kinetics such as Fig. 1. But more often in the researches of real systems have to take place with finite fields where the kinetics of the phase transition is smeared in time and space (Fig. 2), and this requires further study.

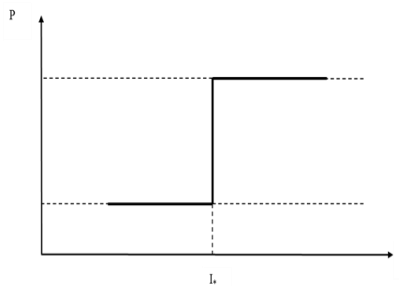


Fig. 1. The phase transition as a critical event

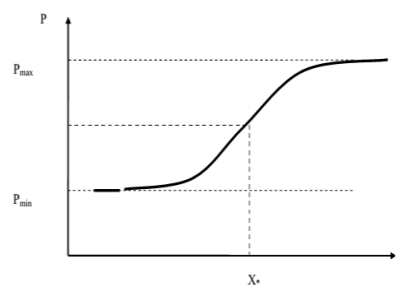


Fig. 2. The phase transition is smeared in time kinetic process

2. Stochastic modeling percolation on finite fields

Modern achievements of percolation theory are widely used in materials, electrical conductivity, filtration theory, chemistry, biochemistry, virology, physics of strength and reliability of structures, information models, models of manipulation of consciousness, etc. [1-6].

The availability of powerful computers and advanced algorithms contribute to the further expansion of interest in the problem of percolation in a variety of areas. However, since such problems connecting the clusters modeling tasks are D - dimensional combinatorics, the theoretical analysis of all possible strumming even for two-dimensional grid of 5×5 contains $\sim 25! \sim 10^{25}$ options, and, of course, is available today are limited to numerical methods. At the same time the task 5×5 or 50×50 do not have much value to practical problems of Strength Physics heterogeneous structures, materials science, nanotechnology, conductivity, meteorology, communication and the like.

On the other hand, the accumulation of a significant amount of numerical simulation results for large values of L should lead to serious theoretical

generalizations, and possibly to the theoretical analysis techniques, as the development method renormalization-group.

Over the past 20 years we have developed a number of algorithms and made significant static percolation study [1-2] in a variety of tasks for $3 \geq D \geq 1$. Fig. 3 shows the results of numerical simulation of percolation on a 3D finite areas to LE [5, 10, 20, 40, 80; 160] made by us to study the effect of scale on the kinetics of the phase transition.

As can be seen from Fig.3, the kinetics of the phase transition depends essentially on the size of the lattice. And not only. The threshold value P^* , at which the phase transition probability $W = 0,5$, also significantly varies with the size of the region L : with L decreasing P^* values are increasing. Using Cartesian approximation prof. Grabar [2]:

$$P^* = 1 - \ln \frac{D+1}{2} \tag{1}$$

where P^* - percolation threshold, D - fractal dimension of the space, it is easy to see that with decreasing L fractal dimension of finite-dimensional regions decreases! It is possible to establish that nanovolumes fractal dimension of the nanoparticles is less than three, may explain their unique properties.

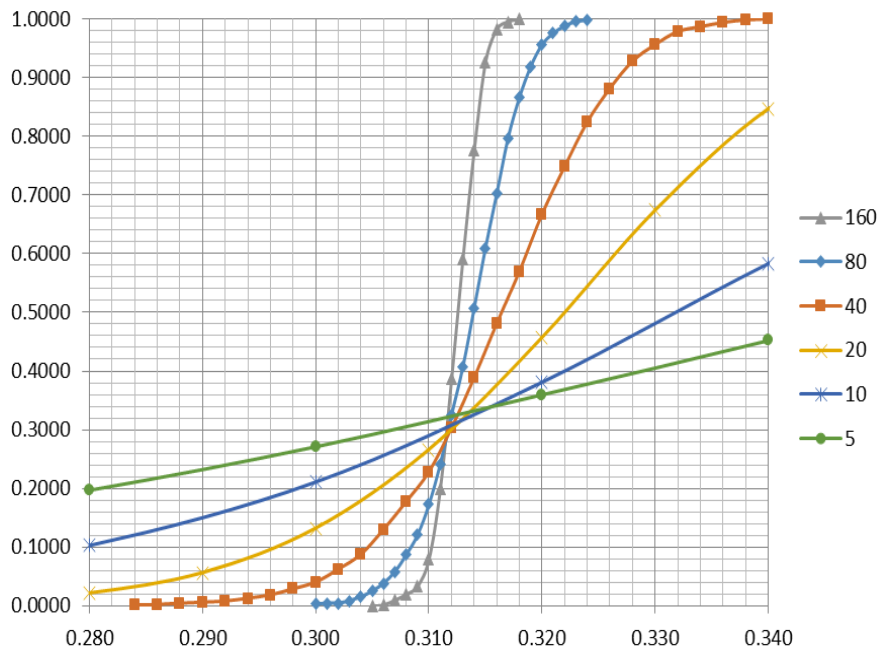


Fig.3. The possibility of connecting cluster $W(P)$ in the 3-D problem percolation when $n = 5, 10, 20; 40, 80; 160$ and 10^6-10^7 repeats for each value of P .

In this blur FI decreased with increasing L. when $L \rightarrow \infty$ phase transition kinetics very close to the stage of Fig. 1 when in passing through the percolation threshold, the value of $p \rightarrow p^*$ occurrence probability cluster connecting changes almost discontinuously:

$$W_{\min} \rightarrow W_{\max}$$

In our case $W_{\min} = 0; W_{\max} = 1$.

In [1-2, 5-6] to approximate the kinetics of AF on finite-dimensional areas we proposed a modified distribution of Fermi- Dirac-Grabar (FDG):

$$W = W_{\min} + \frac{W_{\max} - W_{\min}}{1 + e^{L(P^* - P)}}$$

For normalization of the above conditions ($W_{\min} = 0; W_{\max} = 1$) we have:

$$W = \frac{1}{1 + e^{L(P^* - P)}} \tag{2}$$

When $L \rightarrow \infty$ equation (2) describes a singular "step" type function. In this case L was dependent on not only the slope FP (FP blur width) but also the percolation threshold P^* . The presence of communication between the percolation threshold and the fractal dimension of the space D equation (1) allowed a new role treated percolation threshold P^* in the AF.

Fig.4 shows the percolation threshold on the size L of finite-dimensional region constructed according to Fig. 3:

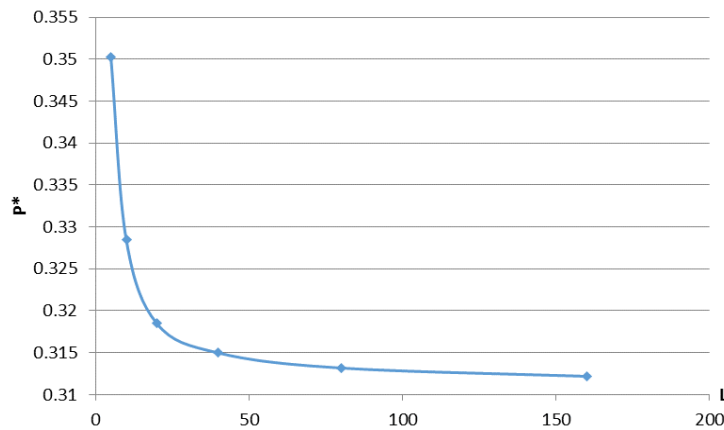


Fig. 4. The dependence of the percolation threshold of size $P^* L$ for 3D nanoparticles

As appears from Fig. 4, at $L > 30 \dots 50$ virtually disappears zoom effect on the percolation threshold P^* .

3. Percolation model of Ferhlyuyst

Let the probability of appearance of new interconnecting clusters W from probability P of the given cell at the predetermined finite-dimensional region described by the Malthus model:

$$\frac{dW}{dp} = L \cdot W \text{ for } p < p^*$$

We define the boundary conditions:

$$W|_{p=0} = 0 \quad W|_{p=p^*} = \frac{1}{2}$$

where:

$$W(p) = \frac{1}{2} e^{L(p-p^*)}$$

However, since the region is finite-dimensional (limited resources available cells), then use the approximation:

$$\left\{ \begin{array}{l} \frac{dW}{dp} = L * W(W_{\max} - W) \\ W|_{p=p^*} = \frac{1}{2} \\ W_{\max} = 1 \end{array} \right. \quad (3)$$

Separate the variables:

$$\frac{dW}{W(1-W)} = Ldp$$

where:

$$\ln \frac{W}{1-W} = Lp + C \quad (4)$$

Substituting in (4) the boundary condition $W|_{p=p^*} = \frac{1}{2}$

then:

$$\ln \frac{\frac{1}{2}}{1 - \frac{1}{2}} = Lp_* + C = \ln 1 = 0$$

from whence $C = -Lp_*$

This allows you to:

$$\ln \frac{W}{1 - W} = Lp - Lp_*$$

after transformation

$$W = \frac{e^{L(p-p_*)}}{1 + e^{L(p-p_*)}}$$

Or, dividing by the numerator, we have:

$$W = \frac{1}{1 + e^{L(p_* - p)}} \tag{5}$$

Thus, we have received a modified version of the Fermi-Dirac distribution. It is worth noting that this type of probability distributions connecting clusters prof. Grabar was [1-2] in numerical studies of percolation. Similar dependences Aliyev [7] used in the study of the kinetics of degradation of phase transitions in semiconductors and objectives of high-temperature superconductivity, as well as in his writings used prof. B. Rolov [8].

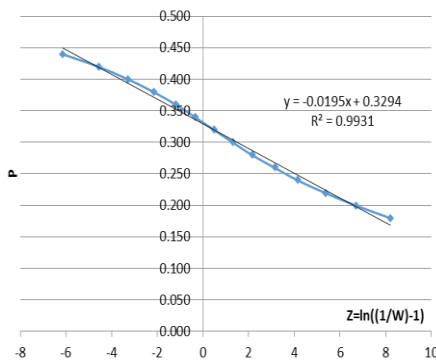


Fig. 5. Simulation: L = 10, D = 3

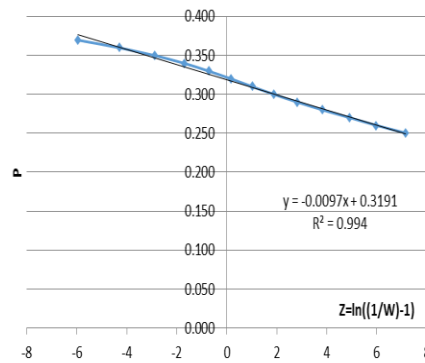


Fig. 6. Simulation: L = 20, D = 3

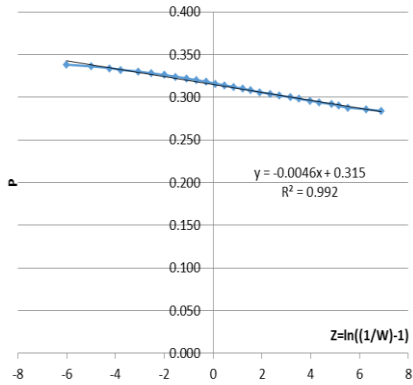


Fig. 7. Simulation: L = 40, D = 3

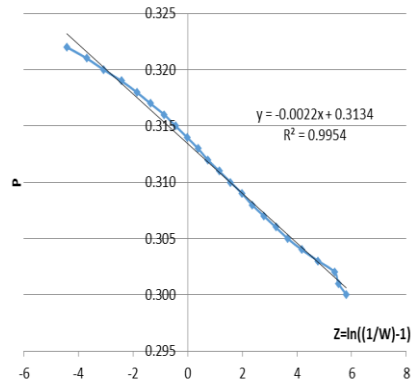


Fig. 8. Simulation: L = 80, D = 3

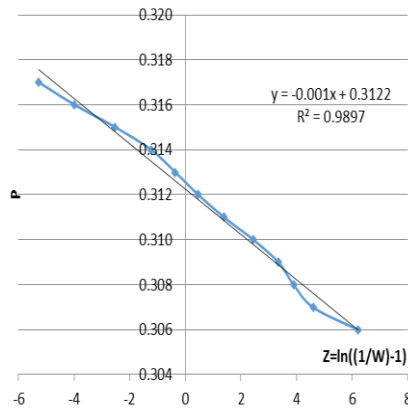


Fig. 9. Simulation: L = 160, D = 3

Fig. 5-9 shows the results of numerical simulation results of the approximation of percolation on a 3D Cartesian areas when L = 10; 20; 40; 80; 160, respectively, relation (5) into the linearized coordinates:

$$P = P^* - \frac{1}{L} \ln\left(\frac{1}{W} - 1\right)$$

High values of the correlation coefficient ($r > 0,99$) suggest that the model (6) adequately describes the kinetics of $W(P)$ - the probability of connecting cluster on finite field in a Cartesian partition. It is easy to see that the solution (5) is a variant of the modified Ferhlyuyt model. It is known that the model Ferhlyuyt worked well in problems of population dynamics in resource-limited settings.

The resulting distribution function $W(p)$ (5) (blurring function percolation phase transition) compared with an accuracy of a Riemann integral (Fig.10) for

the approximation precision of computer simulations (106-107 repeats) occurrence joining the cluster.

As can be seen from Fig. 5-9, we can speak of the equality of data fitting results as a function of (5), and the Riemann integral (integral of the normal distribution function (6):

$$F(x) = \frac{1}{\sigma\sqrt{2\pi}} \int_{-\infty}^x \exp\left[-\frac{(x-\bar{x})^2}{2\sigma^2}\right] dx \quad (6)$$

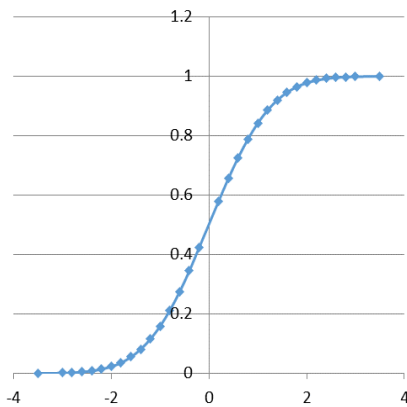


Fig. 10a. Riemann integral (normal distribution) for $x_* = \bar{x} = 0; \sigma = 1$

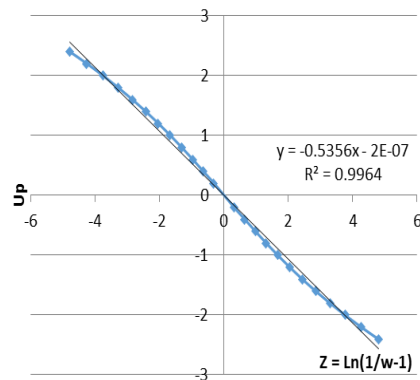


Fig. 10b. Approximation Riemann integral FDG distribution (in the range of values of $Z = [-5, +5]$)

However, for equal values of the reliability forecast (5) has advantages over (6):

- It has a simple and clear physical interpretation;
- easily differentiated and integrated by quadrature's;
- It does not require cumbersome numerical methods;
- allowing when $L \rightarrow \infty$ describe correctly even in the case of AF step (critical conditions).

In addition, the use of statistics FDG (5) for the simulation of random events can explain the physical nature of the ubiquitous spread of normal distribution of random variables, treating it as a result of the internal competition of species in the problems of animate and inanimate nature in resource-limited settings.

Fig. 11 shows the 3D fractal dimension of the nanoparticles on their size, obtained by processing of the numerical simulation results and Cartesian approach prof. Grabar (1). Depending on the Fig. 11 can be divided into two fundamentally different areas:

$$I - L \leq L_*$$

$$II - L > L_*$$

The L_* value of the correlation radius we called percolation. For $D \sim 3$

$$L_* \sim 30...50$$

Thus, for most metals lattice parameter $a_0 \sim 2 \dots 5 \text{ \AA}$, The characteristic size of the nanoparticles:

$$d_* \approx L \cdot a_0 \approx (60...250) \text{ \AA}$$

which is close to the actual size of nanoparticles, and can give some explanation of the physical features of the behavior of nanomaterials. From this perspective, there is an increased interest in obtaining the function $P^*(L)$ from first principles, but now our efforts have not been successful.

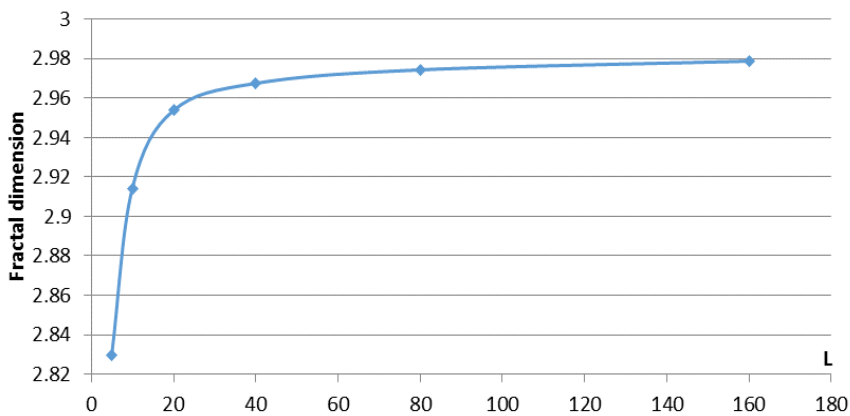


Fig.11. The fractal dimension of the nanocluster $L \times L \times L$

When $L \geq L_*$ a further increase in the field does not affect the fractal dimension of nanoclusters (Fig. 11). Thus, $L = L_*$, the title correlation radius is a threshold finite field above which does not alter the kinetics of the process. The kinetics of the objects animate and inanimate nature is a large number of analogues: a critical mass of uranium in a nuclear reaction; the maximum number of friends - the number of Dunbar, the limiting density of population (PT breeding locusts, swarming bees etc.); flashpoint fuel, the critical mass of snow on a mountain slope, leading to avalanche etc.

Fig.12 shows the dependence of the percolation threshold of the value of the width of the strip length L (a) and layer thickness $L \times L$. Firstly, the graphics update data demonstrate percolation threshold P^* with a smooth transition from $D = 1$ to $D = 2$ (a) and from $D = 2$ to $D = 3$ (b). Their comparison with Fig.4 and Fig. 11 shows the kinetics of similarity. Secondly, the presence of dependencies

and Fig. 12 Cartesian approximation prof. Grabar (1) enable for a given P^* determine fractal dimension of any quasi-fractal.

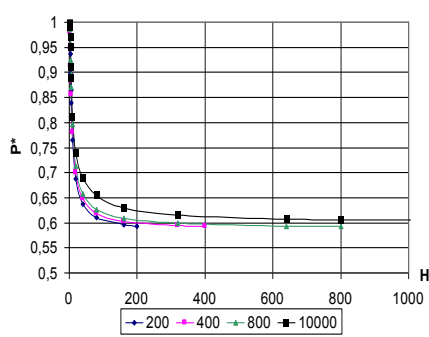


Fig. 12a. R^* changes depending on the layer thickness for space $R1 \rightarrow R2$ for $L = 200, 400, 800, 10000$; for $L = 200$, $P^*(H) = 0,483 \cdot H^{-0,442} + 0,59$

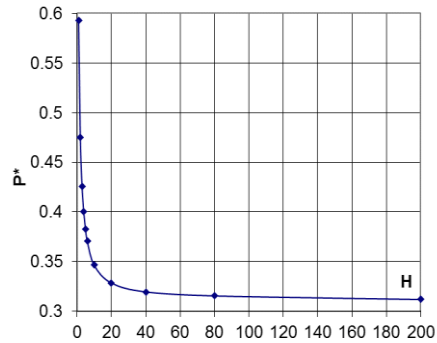


Fig. 12b. R^* changes depending on the layer thickness for the space from $R2 \rightarrow R3$ for $L = 200$, $P^*(H) = 0,286 \cdot H^{-0,845} + 0,31$

Fig. 13-15 [9-12], the number depending on the melting point of metallic nanomaterials on the nanoparticle size and revealed similarity of these kinetics dependencies Fig. 4, Fig. 11 and Fig. 12:

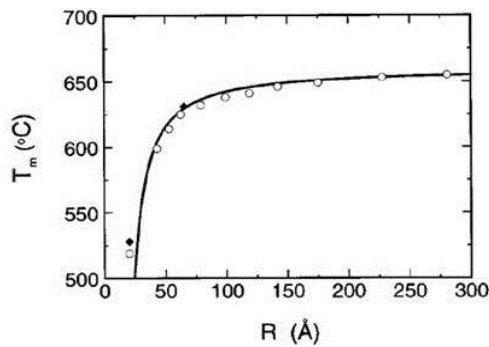


Fig. 13. The melting point of the aluminum nanoparticles on their radius (Recovered from Lai et al Applied Physics Letters, 1998, v. 72, 1098-1100).

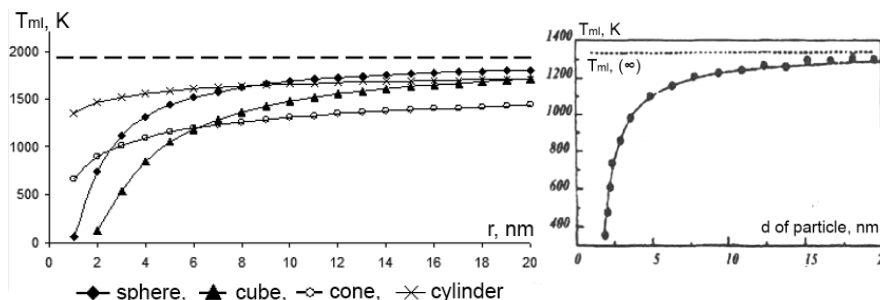


Fig. 14 Dependence of the melting temperature of titanium nanoparticles of size and geometric shape (r - for the scope of - the radius of a cube - the rib, for the cone - the height of the cylinder - height) [10]

Fig. 15. The dependence of the melting temperature of gold nanoparticles on their size [12]

Conclusions

1. Statistical modeling percolation confirm the accuracy of the Cartesian approach prof. Grabar of the functional dependence of the percolation threshold of the fractal dimension of the space: $P_* = 1 - \ln((D + 1)/2)$ and discloses a deep physical relationship between fractal dimension space and percolation threshold in this space.
2. Modeling of W(P) on finite models allows to show that for typical nanoparticles sizes of $d \leq (30 \dots 50) a_0$ - their fractal dimension is less than three ($D < 3$), which allows a new approach to the explanation of phenomenal properties of nanoparticles and nanomaterials.
3. The mathematical simplicity (5), the possibility of a quadrature analysis the forward and inverse problems of the statistical analysis is an additional incentive for application distribution FDG study both phase transition kinetics, and to study the problems of random variables, especially - in multidimensional problems and limited statistical samples.
4. The similarity of the fractal dimension kinetics dependency of nanoparticle-scale finite-dimensional region and the melting temperature of the scale of nanoparticles is a consequence of the fractal dimension on the melting temperature.
5. Distribution of FDG is not only quantitatively describes the distribution of the random value close to the normal distribution, but also to explain the physical nature of this "normality", as a consequence of the growth of percolation clusters (or their equivalent) in the conditions of competition for scarce resources.

References

1. Grabar I.G., Grabar O.I., Gutnichenko A.A., Kubrak Y.A. Percolation-fractal materials, Zhytomyr, ZSTU, 2007, 354 pages. (in Ukrainian)
2. Grabar I.G. Percolation-fractal model in a modern material science, Scientific notes of LNTU, Lutsk, 2015. (in Ukrainian)
3. Grabar I.G. Thermoactivation analysis and synergetic destruction, Zhitomir, ZITI, 2002, 312 pages. (in Ukrainian)
4. Grabar I.G., Grabar O.I. Modeling of kinetics of randomization and Feigenbaum attractor dynamics of nonlinear systems, ZSTU, No. 3, 2012. (in Ukrainian)
5. Grabar I. G. MACROMODEL interaction between atoms of the alloying elements to the matrix, In the book: Reports of the International scientific - practical conference "rheological models and processes deformation structure - heterogeneous materials.", Lutsk, LNTU, 2016.
6. Grabar I.G., Grabar O.I., Degtar Y.D. Biocompatible porosity ceramics induced surface charge and design water filter.: Advanced technology, technology and engineering education. 17 International scientific-practical conference, Kiev-Odessa, 2016.
7. Aliev S.A. The smearing of phase transitions in semiconductors and high-temperature superconductors. Monografy. Baku, Elm, 2007, 286 pages.
8. Rolov B.N. Blur phase transitions Riga, 1972, 311 pages.
9. Alymov A.I., Shorshorova M.H. Effect size factor at the melting point and surface tension of ultrafine particles, Izv.RAN. Metals. 1999, No. 2, 29{31.
10. Beznosyuk S.A., Bandini A.E. Computer modeling of melting a spherical metal nanoparticles // polyfunctional chemical materials and technologies: Proc. articles. - Tomsk, 2007, Volume 1.
11. Golovenko J.V., Gafner S.L., Gafner Y.Y. Investigation of structural states of gold nanoclusters by molecular dynamics. // Proceedings of the universities. Physics. -. 2008, Volume 51, No. 11/3, 186{190.
12. Ph.Buffat, J.-P.Borei. Size effect on the melting temperature of gold particles // Phys.Rev., 1976, v. 13, 2287{2298.